Plant Molecular Biology (2025) 115:20
https://doi.org/10.1007/s11103-024-01547-5

Time-series transcriptome analysis reveals the cascade mechanism of biological processes following the perturbation of the MVA pathway in *Salvia miltiorrhiza*

Fang Liu[1] · Nan Li[1] · Zhu-Yun Yan[1] · Xin Chen[1]

Received: 25 May 2024 / Accepted: 13 December 2024 / Published online: 17 January 2025

Abstract

Various biological processes are interconnected in plants. Transcription factors (TFs) often act as regulatory hubs to regulate plant growth and responses to stress by integrating various biological pathways. Despite extensive studies on TFs functions in various plant species, our understanding of the details of TFs regulation remains limited. In this study, clonal seedlings of *Salvia miltiorrhiza* were exposed to specific inhibitors for 12 h. Time-series transcriptome data, sampled hourly, were used to construct co-expression networks and gene regulatory networks (GRNs). Transcriptome dynamic analysis was utilized to capture the gene expression dynamics of various biological processes and decipher the potential molecular mechanisms that regulate these processes. The perturbation results showed the growth and development processes of *S.miltiorrhiza* were primarily affected at the early stage, whereas stress response-related biological processes were mainly influenced at the later stage. And there was a correlation between the series of key differentially expressed genes in terpenoid biosynthesis pathways and the topological distribution of these pathways. Furthermore, the GRNs based on TFs indicate that TFs play a crucial role in connecting various biological processes. In the cytoplasmic lysate gene regulatory module, *Sm*WRKY48-*Sm*TCP*4*-*Sm*WRKY28 constituted a regulation hub regulating *S.miltiorrhiza* responses to perturbation of the MVA pathway. The regulation hub mediated various pathways, including pyruvate metabolism, glycolysis/gluconeogenesis, amino acid metabolism, and ubiquinone and other terpenoid-quinone biosynthesis.Our findings suggest that perturbation of a key biological pathway in *S.miltiorrhiza* has time-dependent effects on other biological processes. And *Sm*WRKY48-*Sm*TCP4-*Sm*WRKY28 constitutes the regulatory hub in *S.miltiorrhiza* responses to perturbation of MVA pathway.

Key message

After disrupting the MVA pathway in *Salvia miltiorrhiza* with specific inhibitors, a gene regulatory network involving transcription factors reveals a potential mechanism for the synergistic effects of interconnected biological processes.

Introduction

Various biological processes are interconnected in plants. This connection is mediated through multiple molecular mechanisms. In contrast to other regulators like long non-coding RNAs (lncRNAs), microRNAs (miRNAs), and hormones, transcription factors (TFs) demonstrate a complex regulatory association with their target genes. Many TFs display a multi-to-multi regulatory pattern, enabling them to concurrently regulate multiple target genes involved in diverse biological processes (Shen-Orr et al. 2002). This characteristic of TFs promotes the interconnectedness among various biological processes. TFs often act as the regulatory hubs regulating plant growth and responses to

✉ Xin Chen
chenxin@cdutcm.edu.cn

Fang Liu
liuyunxia@stu.cdutcm.edu.cn

Nan Li
linan@stu.cdutcm.edu.cn

Zhu-Yun Yan
yanzhuyun@cdutcm.edu.cn

[1] School of Pharmacy, Chengdu University of Traditional Chinese Medicine, Chengdu, Sichuan, China

stress through integrating various pathways. For instance, UB2/UB3/TSH4 acted as the signaling hubs regulating inflorescence development through integrating light and hormone signaling pathways in *Arabidopsis thaliana* (Kong et al. 2023).

The MYB-bHLH-WD40 regulatory complex controlled anthocyanidin biosynthesis in *Vaccinium corymbosum* fruit and color development (Zhao et al. 2019). The HSF, WRKY, and bZIP transcription factor families could regulate various biological processes in *Pinellia ternata* under shade conditions, including the accumulation of reactive oxygen species, light signals, and programmed cell death (Yang et al. 2023). Transcription factor families such as MYB, bHLH, and NAC coordinated the interplay among the biosynthesis processes of secondary metabolites like flavonoids, caffeine, and theanine in tea trees (Li et al. 2015a).

Studies have shown that plants exhibit multiple temporal scales at different regulatory levels when faced with external stimuli. Transcriptional regulation can occur in minutes or hours (Li et al. 2015b). Therefore, conducting a temporal transcriptome analysis over hours would be more beneficial for capturing dynamic events in gene transcriptional regulation, thus revealing the regulatory relationships between genes in a specific biological state. Time-sequence-based transcriptomes are preferred for constructing gene co-expression networks (GCNs) and gene regulatory networks (GRNs) (Alvarez et al. 2021). For example, to investigate the molecular mechanism of salt stress tolerance in *Aquilegia vulgaris*, a time series transcriptome analysis was conducted. Samples were collected after exposure to NaCl treatment for 0, 12, 24, and 48 h. The results showed that plant responses to salt stress involved cell wall composition and metabolism-related biological processes. Further analysis by constructing GRNs has revealed that the AP2, MYB, and bHLH transcription factor families might play crucial roles as key regulators in plant responses to salt stress (Bai et al. 2023). To address the challenge of predicting causal relationships between TFs and their target genes, various algorithms have been developed to construct GRNs, including ARACNE (Algorithms for Reconstruction of Accurate Cellular Networks) (Margolin et al. 2006), CLR (Context Likelihood of Relatedness) (Faith et al. 2007), GENIE3 (Gene Network Inference with Ensemble of Trees 3) (Huynh-Thu et al. 2010), TIGRESS (Trustful Inference of Gene REgulation using Stability Selection) (Haury et al. 2012), and other methods. It has been discovered that no single method for GRN inference performs optimally across all datasets. Combinations of different method strategies often demonstrate robustness and superior performance in network inference, a phenomenon known as the "wisdom of the crowds" (Marbach et al. 2012). Specifically, bioNERO (Almeida-Silva and Venancio 2022), an all-in-one R-package that encompasses all stages of the network analysis process, applies the "wisdom of the crowds" approach to constructing GRNs. It integrates three popular GRN inference algorithms—GENIE3, ARACNE, and CLR.

In plants, isoprenoids, also known as terpenes or terpenoids, are one of the most diverse organic compounds found in nature. They include primary products such as chlorophyll, carotenoids, ubiquinone, cytokines, gibberellin, oleuropein steroids, and abscisic acid, as well as numerous secondary metabolites with medicinal value, such as tanshinone, paclitaxel, artemisinin, and ginsenoside (Pichersky and Raguso 2018; Krause et al. 2023). Isoprenoids play a crucial role in growth, development, and stress responses. The mevalonic acid pathway (MVA) produces cytosolic isopentenyl diphosphate (IPP), while the methylerythritol pathway (MEP) generates IPP and its isomer dimethylallyl diphosphate (DMAPP) in plastids (Rohmer and Rohmer 1999). Changes in the expression of genes, the stability of proteins, and the activity of enzymes in either of these two pathways can affect a wide range of biological processes in plants (Cho et al. 2022). For example, it was found that treating *Trigonella foenum-graecum* with a specific inhibitor of HMGR (3-hydroxy-3-methyl glutaryl coenzyme A reductase) for 72 h significantly inhibited root growth and resulted in a approximately 50% decrease in diosgenin content (Cao et al. 2021). Overexpression of *Md*HMGR5 (from *Malus pumila*) in *Arabidopsis thaliana* enhanced the antioxidant stress capacity of the plant (Zhang et al. 2020). It suggests that when the MVA pathway is perturbed, multiple other biological processes will be affected.

Salvia miltiorrhiza is an important medicinal plant, with terpenoids and phenolic acids being its main medicinal components. Biological processes related to terpenoids have been extensively studied (Gao et al. 2014; Lu et al. 2022). This makes *S.miltiorrhiza* a valuable material for in-depth study of the role of the isoprenoid biosynthetic pathway in regulating plant metabolism and its relationship with other related pathways. In this study, we utilized lovastatin (LOV), a specific inhibitor of HMGR, to treat *S.miltiorrhiza* clonal seedlings. Subsequently, we conducted a dynamic transcriptome analysis. By constructing GCNs and GRNs, we have revealed the changing sequence of relevant biological processes and their underlying mechanisms following the perturbation of the MVA pathway.

Materials and methods

Plant materials and growing conditions

Leaf explants were obtained from potted *S.miltiorrhiza* from the seed source of Zhongjiang County, Sichuan Province,

China. The explants were then were used to induce callus formation and organogenesis (Tsai et al. 2015). Well-developed seedlings were transplanted into a series of MS (Murashige and Skoog 1962) medium. Then the cultures were incubated in a growth chamber with a 14/10 h (light/dark) photoperiod and a temperature of 24 ± 2 ℃.

Treatment of *S.miltiorrhiza* clonal seedlings with the inhibitor LOV

The activation of LOV and the preparation of stock solutions were conducted according to Hagen's methods (Hagen and Grunewald 2000). For time series analysis, seedlings were treated with (i) MS medium containing the LOV solution with final working concentrations of 10 µM (Blazquez et al. 2012) or (ii) LOV free MS medium at 6:00 a.m. Triplicate root samples, both treat and control, were harvested at 2, 4, 6, 8, 10, and 12 h after treatments. All samples were stored at – 80 °C for RNA sequencing and HMGR activity assay. For concentration gradient test, seedlings were treated with 0 µM, 10 µM, 50 µM, 100 µM, and 200 µM final working solution concentrations of LOV respectively at 6:00 a.m. After 12 h (at 6:00 p.m), triplicate root samples were collected. All samples were stored at – 80 °C for RNA sequencing.

Total RNA extraction, library construction, sequencing and alignment

Total RNA was extracted from the roots using the MJZol Total RNA Extraction Kit (Majorbio Bio-Pharm Technology, Shanghai, China) following the manufacturer's instructions. Then, RNA quality was determined using the 5300 Bioanalyser (Agilent) and quantified with the ND-2000 (NanoDrop Technologies). Only high-quality RNA sample (OD260/280 = 1.8 ~ 2.2, OD260/230 ≥ 2.0, RQN ≥ 6.5, 28S:18S ≥ 1.0, > 1µg) was used to construct the sequencing library. RNA purification, reverse transcription, library construction, and sequencing were conducted at Shanghai Majorbio Bio-pharm Biotechnology Co., Ltd. (Shanghai, China) following the manufacturer's guidelines. The RNA-seq transcriptome library was prepared following Illumina® Stranded mRNA Prep Ligation (San Diego, CA). The sequencing library was prepared using the NovaSeq 6000 platform (PE150) and the NovaSeq Reagent Kit.

The raw paired-end reads were trimmed and quality-controlled using fastp (Chen et al. 2018) with default parameters. In this step, clean data was obtained by removing read segments containing artifacts and low-quality reads from the raw data. All subsequent analyses were based on high-quality, clean reads. Clean reads were separately aligned to *S.miltiorrhiza* reference genome in orientation mode using HISAT (Kim et al. 2015). The reference genomes and gene annotations for chromosome-level genomes were downloaded directly from the website (https://ngdc.cncb.ac.cn/gwh/Assembly/10381/show) (Song et al. 2020).

Differential expression analysis and functional enrichment

Gene expression was quantified using RNA-Seq via Expectation–Maximization (RSEM) (Li and Dewey 2011) and then normalized by transcripts per kilobase per million mapped reads (TPM) values. Differential expression analysis was performed using the DESeq2 package (Love et al. 2014). To investigate the changes in the transcript abundance following LOV treatment, TPM values were utilized to calculate the gene expression level in the LOV-treated samples compared to the control samples. A gene was considered to be differentially expressed when it displayed an absolute value of log2 (fold change) ≥ 1 and an adjusted P-value < 0.5.

In addition, functional annotation of the differentially expressed genes (DEGs) was conducted using the gene ontology (GO) database (http://www.geneontology.org) and the Kyoto Encyclopedia of Genes and Genomes (KEGG) database (http://www.genome.jp/kegg/). Functional enrichment analysis, including GO and KEGG, was conducted to determine which DEGs were significantly enriched in various GO terms and metabolic pathways. GO functional enrichment and KEGG pathway analysis were conducted using Goatools and KOBAS software (Young et al. 2010; Kanehisa et al. 2008).

HMGR activity assay

The roots of clonal seedlings were harvested after LOV treatment for 2, 4, 6, 8, 10, and 12 h. Samples weighing 0.1 g were used for enzyme assays following the protocol outlined in the Plant HMGR ELISA KIT (Lunchangshuo Biotechnology, China).

Construction of GRNs

To obtain comprehensive gene functional information, the assembled transcriptome was annotated through BLAST searches against several databases, including Nr (Non-Redundant Protein Sequence Database) (https://www.ncbi.nlm.nih.gov/public/), eggNOG (Evolutionary Genealogy of Genes: Non-supervised Orthologous Groups) (http://eggnogdb.embl.de/#/app/home), Pfam (http://pfam.xfam.org/), GO (http://www.geneontology.org), KEGG (http://www.genome.jp/kegg/), and Swiss-Prot (http://web.expasy.org/docs/swiss-prot_guideline.html). TFs were screened based on the annotation

information and classified according to PlantTFDB v5.0 (http://planttfdb_v4.cbi.pku.edu.cn/). TFs with normalized expression values (TPM) ≥ onefold change and an adjusted P-value < 0.5 were considered as differentially expressed TFs. Based on the GO annotation information, the DEGs annotated to the same cellular components, such as chloroplast, mitochondria, endoplasmic reticulum, Golgi apparatus, and cytoplasmic lysosome, were grouped into a gene set. GRNs were constructed based on differentially expressed TFs and DEGs in the gene set using bioNERO. Gephi (Bastian et al. 2009) was used for visualizing GRNs and filtering the top 5 hub genes.

Construction of GCNs

The R package WGCNA (Weighted Gene Co-expression Network Analysis) (Langfelder and Horvath 2008) was used to construct GCNs. Firstly, the bioNERO R script was used to preprocess the gene expression data to remove the low expression data (TPM < 1). The outlier samples were then removed using the standardized connectivity method. Based on the topological overlap (TOM) dissimilarity, genes were clustered using the average-link hierarchical clustering method. The gene modules were determined using the dynamic cutting method. The correlation between the eigengene vector of the obtained module and the HMGR concentration of the sample was calculated using the function module-TraitCor. The module with the maximum correlation coefficient was chosen as the module significantly associated with HMGR concentration. The function expor-NetworkToCytascape was used to export the edge and node information of genes in each module. Finally, networks were visualized using Cytoscape v3.9.1 (Shannon et al. 2003) and the top 10 hub genes in the networks were calculated using the Maximum Clique Centrality algorithm (Chin et al. 2014).

Quantitative real-time PCR verified selected genes

Total RNA was isolated using the Plant Total RNA Extraction kit (Foregene Biotech, Chengdu, China) and then treated with DNase I. First-strand cDNA was synthesized from the total RNA using the De-etiolated First-strand cDNA Synthesis Kit (Foregene Biotech, Chengdu, China). Quantitative real-time PCR (RT-qPCR) and data analyses were performed as previously described (Jiang et al. 2020) and the $2^{-\Delta\Delta CT}$ method (Livak and Schmittgen 2001) was used to calculate the relative abundance of selected genes. All primers were designed using Primer Premier 6 (Singh et al. 1998) and synthesized by Tsingke Biotech Co., Ltd. All primers used are listed in Table S1.

Results

Complex variation of DEGs number at different sampling time points

The standardized expression values (TPM) of genes in *S.miltiorrhiza* samples treated with LOV for 2, 4, 6, 8, 10, and 12 h are presented in the Table S2. At each sampling time point, genes with the TPM ≥ twofold change and an adjusted P-value < 0.5, compared with the control group, were considered as differentially expressed genes. Based on these criteria, a total of 748, 228, 239, 434, 887, and 1661 DEGs were identified after LOV treatment for 2, 4, 6, 8, 10, and 12 h, respectively. The sample treated with LOV for 12 h showed the highest number of DEGs (Fig. 1). The shared DEGs among the samples at different time points show complex relationships, as shown in Fig. 1 for details. It has also been observed that when *S.miltiorrhiza* was first exposed to LOV, there was a period of rapid and significant changes in gene expression within a short timespan of 2 h. Subsequently, the number of DEGs exhibited a tendency to gradually increase over time.

Different biological processes enriched by DEGs

The DEGs were analyzed by GO enrichment to characterize their functions at each sampling time points. The significantly enriched GO terms were identified based on the criterion of a P-value < 0.05 (Fig. 2a–f). The top 10 significantly enriched GO terms in the biological process (BP) category at each time point are presented in Table S3. The results indicated that the BPs varied significantly at different time points. Among these BPs, the terms with the most DEGs at each time point were, in the following order: "carbohydrate metabolic process" (GO:0005975, 2 h, 46 DEGs), "terpene biosynthetic process" (GO:0016114, 4 h, 8 DEGs), "lipid X metabolic process" (GO:2,001,289, 6 h, 2 DEGs), "RNA processing" (GO:0006396, 8 h, 25 DEGs), "isoprenoid biosynthetic process" (GO:0008299, 10 h, 18 DEGs), "metabolic process" (GO:0008152, 12 h, 504 DEGs).

Different pathways enriched by DEGs

KEGG is a knowledge base for the systematic analysis of gene functions, linking genomic information with higher-order functional information (Kanehisa and Goto 2000). In this study, the DEGs were further analyzed using KEGG enrichment. The results showed that DEGs could be assigned to 26 pathways, separately. Among these pathways, 24 pathways were related to metabolism. It indicated that the inhibitor primarily affected plant metabolism. After the 2, 10

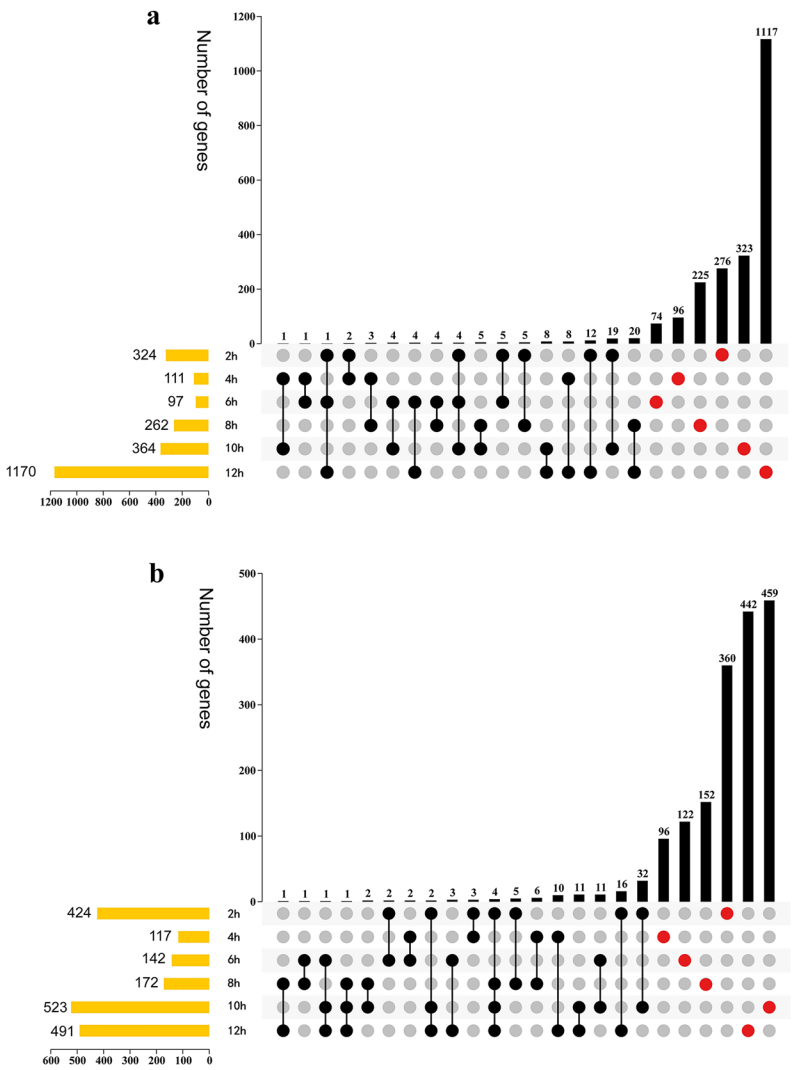

Fig. 1 The DEGs at different time points **a**. upset plot shows the number of up-regulated DEGs; **b** upset plot shows the number of down-regulated DEGs. The upper part of the bar graph indicates the expression pattern of DEGs at different time points, and the total number of genes up-regulated and down-regulated at each time point is shown on the left side. "2 h", "4 h", "6 h", "8 h", "10 h", and "12 h" indicate that the samples were collected after LOV treatment for 2 h, 4 h, 6 h, 8 h, 10 h, and 12 h

and 12 h of LOV treatment, "photosynthesis (map00195)" was significantly enriched. "Inositol phosphate metabolism (map00562)" was significantly enriched at 2 h and 4 h. "Biosynthesis of various plant secondary metabolites (map00999)" and "tyrosine metabolism (map00350)" were significantly enriched at 2 h and 12 h (Fig. 3). The descriptions of different pathway IDs are presented in Table S4.

Notably, DEGs enriched in various terpenoid biosynthesis-related processes at different time points. For instance, "monoterpenoid biosynthesis (map00902)" was significantly enriched in the samples treated with LOV for 2 h; "diterpenoid biosynthesis (map00904)" and "zeatin biosynthesis (map00908)" were significantly enriched at 4 h; "carotenoid biosynthesis (map00906)" was significantly enriched at 6 h; "sesquiterpenoid and triterpenoid biosynthesis (map00909)" and "terpenoid backbone biosynthesis (map00900)" were significantly enriched at 10 h (Fig. 3). This suggests that when plants are disturbed by LOV, the order of influence on terpenoid biosynthesis-related pathways is related to the topological relationship among these pathways. Interestingly, the effect on "terpenoid backbone biosynthesis (map00900)" occurs at the late stage.

Differential expression of TFs at different sampling time points

TFs play crucial roles in regulating plant growth and development, as well as in responding to environmental stresses. In this experiment, a total of 79 differentially expressed TFs were identified in the samples treated with LOV, involving 19 transcription factor families, namely bHLH, bZIP, C2H2, WOX, HSF, MADS, MYB, NF-YA, AT-hook, GRAS, AP2/ERF, NZZ/SPL, Nin-like, SRS, TCP, WRKY, ZF-HD, BES1, and PDGFA Associated Protein 1 (Fig. 4a). The one with the highest number of differentially expressed TFs was the AP2/ERF family, comprising a total of 16 differentially expressed TFs (Fig. 4a).

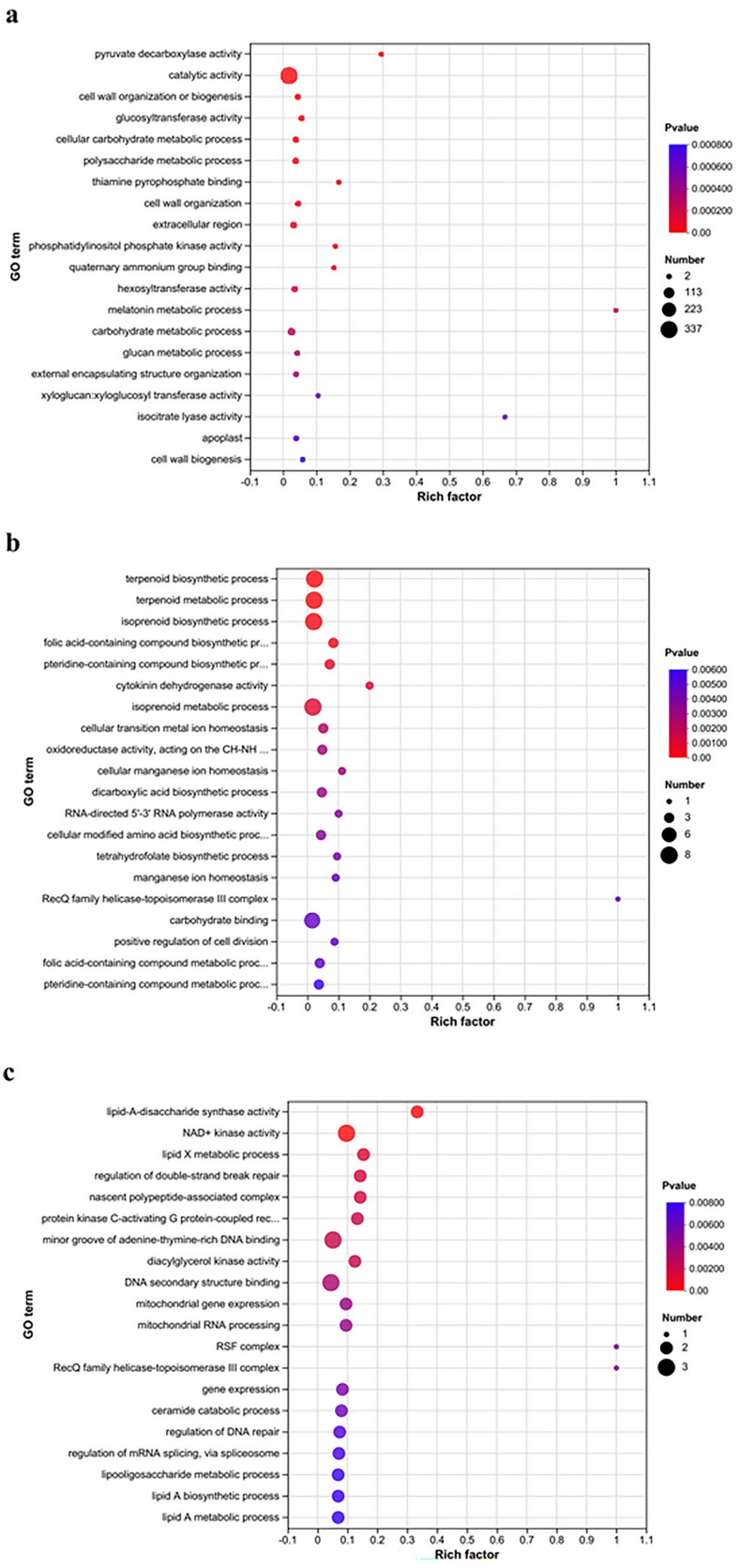

Fig. 2 Bubble plots of GO enrichment for DEGs at different times **a**–**f**. Top 20 significantly enriched GO terms at 2 h, 4 h, 6 h, 8 h, 10 h, and 12 h

Fig. 2 (continued)

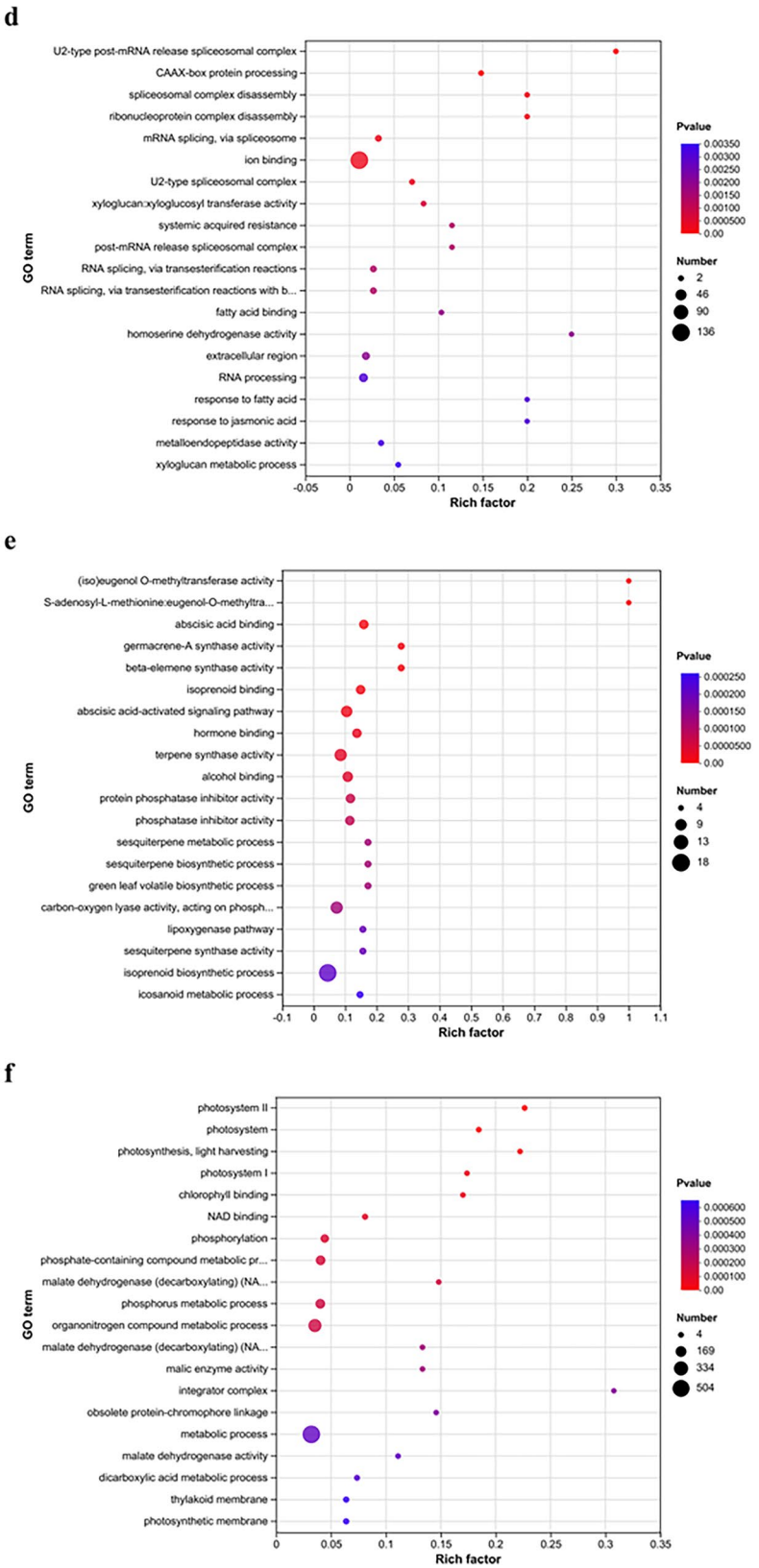

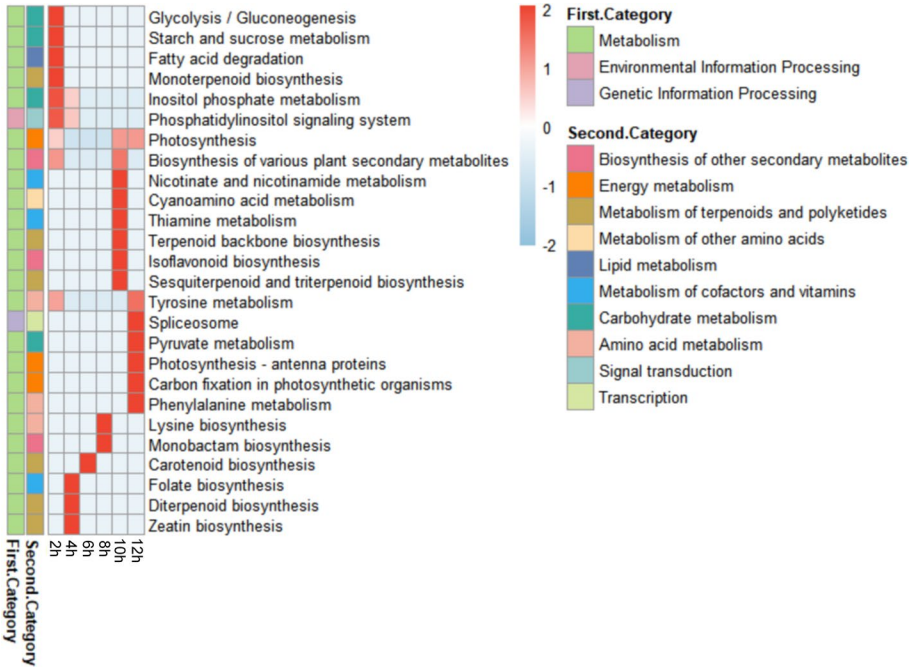

Fig. 3 KEGG pathways significantly enriched in DEGs at different time points Heatmap based on the number of DEGs enriched in each pathway at different times

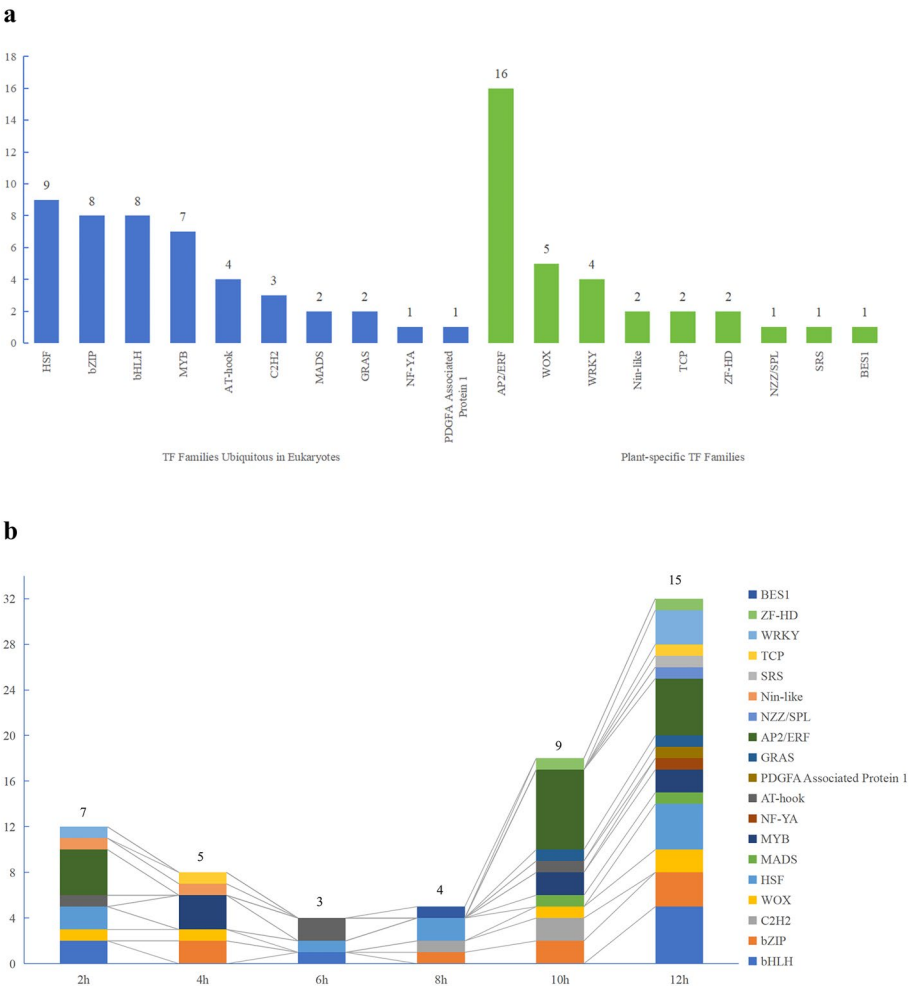

Fig. 4 The differentially expressed TFs at each time point a. Statistics of the number of differentially expressed TFs, the height of the bar indicates the number of members in the transcription factor family, the blue bar indicates the transcription factor families prevalent in eukaryotes, and the green bar indicates the transcription factor families specific to plants; b. Changes of differentially expressed transcription factor families at different time points, the height of the bar indicates the number of TFs, and the number above indicates the number of transcription factor families

The results also showed that the TFs were expressed differentially at various time points. The sample with the most transcription factor families in differentially expressed genes was taken from the 12th hour (Fig. 4b). AT-hook and Nin-like families were predominantly differentially expressed in the early phase, while bHLH, HSF, AP2/ERF, and WRKY families were predominantly differentially expressed in the late phase. Some transcription factor families are expressed differentially at multiple time points. For example, the WOX family was differentially expressed at 2, 4, 10, and 12 h; the HSF family was differentially expressed at 2, 6, 8, and 12 h; the bZIP family was differentially expressed at 4, 8, 10, and 12 h. *Sm*WOX11-like, a member of the WOX family, was significantly differentially expressed in the samples treated with LOV for 4, 10, and 12 h. Details of the differentially expressed TFs at different time points are shown in Table S5.

Active expression of different gene sets at different sampling time points

To investigate the co-expression dynamics of genes, a weighted gene co-expression network analysis was conducted. Total 116 co-expressed modules were identified. Among them, the turquoise module was the largest, containing 8679 genes, while the steelblue and salmon modules showed a strong correlation with HMGR concentration (Fig. S1) (P-value < 0.05, Fig. 5a–c). The HMGR concentrations of samples at different sampling time points are shown in Fig. S2. The top 10 hub genes in the three modules were identified by analyzing nodes with centrality in the largest clusters (Table S6). Functional enrichment analysis of the three gene modules based on GO and KEGG was conducted to elucidate the underlying biological functions of these genes within their networks.

The genes of these three modules were enriched in various GO terms of biological process category. The top 20 significantly enriched GO terms are shown in Fig. 6 (P-value < 0.05). The enriched terms indicated that the turquoise module was primarily associated with gene transcription-related biological processes. The steelblue and salmon modules were mainly related to the biological processes of macromolecular biosynthesis and glucose metabolism (Table S7).

The KEGG enrichment analysis revealed that genes of turquoise, steelblue and salmon module can be categorized into 17, 27 and 24 pathways (P-value < 0.05) (Fig. 7). There were 9 of 17 pathways related to the genetic information processing in turquoise module. Analysis of the expression profiles of the top 10 hub genes in this module revealed that the peak expression of these genes occurred at hour 8 (Fig. S3a). It was indicated that the genes involved in genetic information processing biological processes were actively

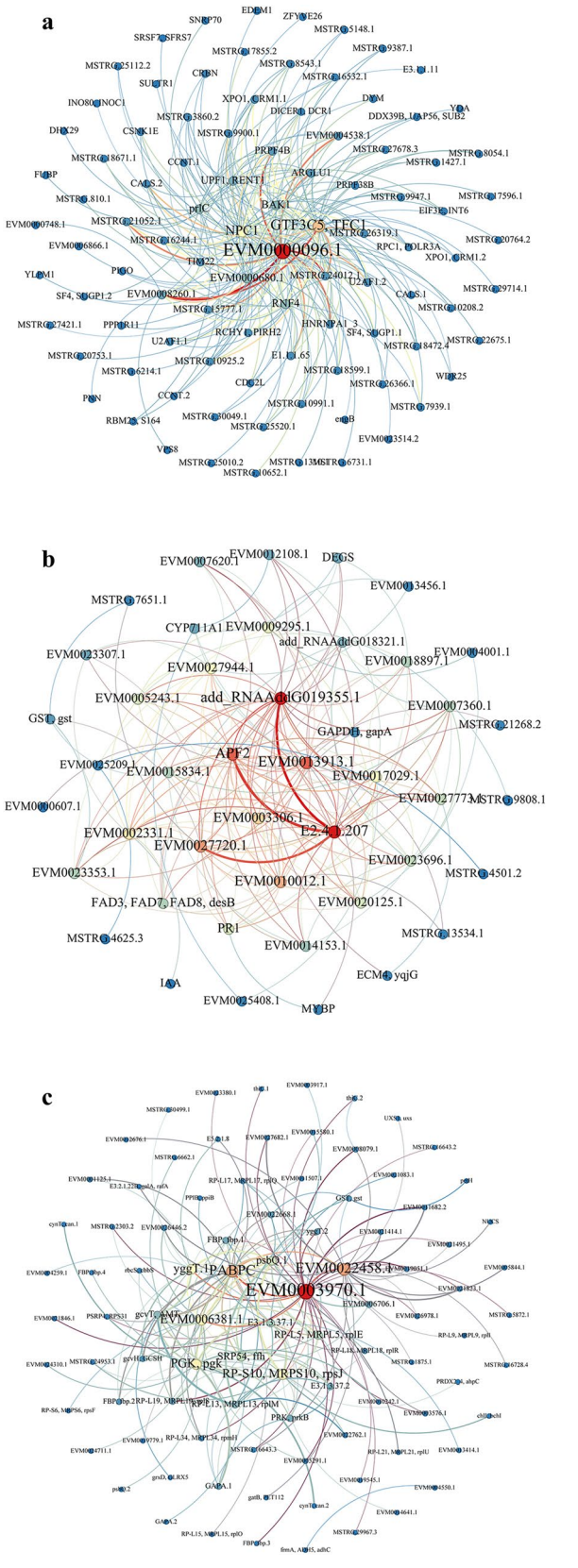

Fig. 5 Co-expression network which were constructed based on the genes of the turquoise (**a**), steelblue (**b**), and salmon (**c**) modules. The central genes in the network are indicated by red color, and the bigger the node, the higher the centrality

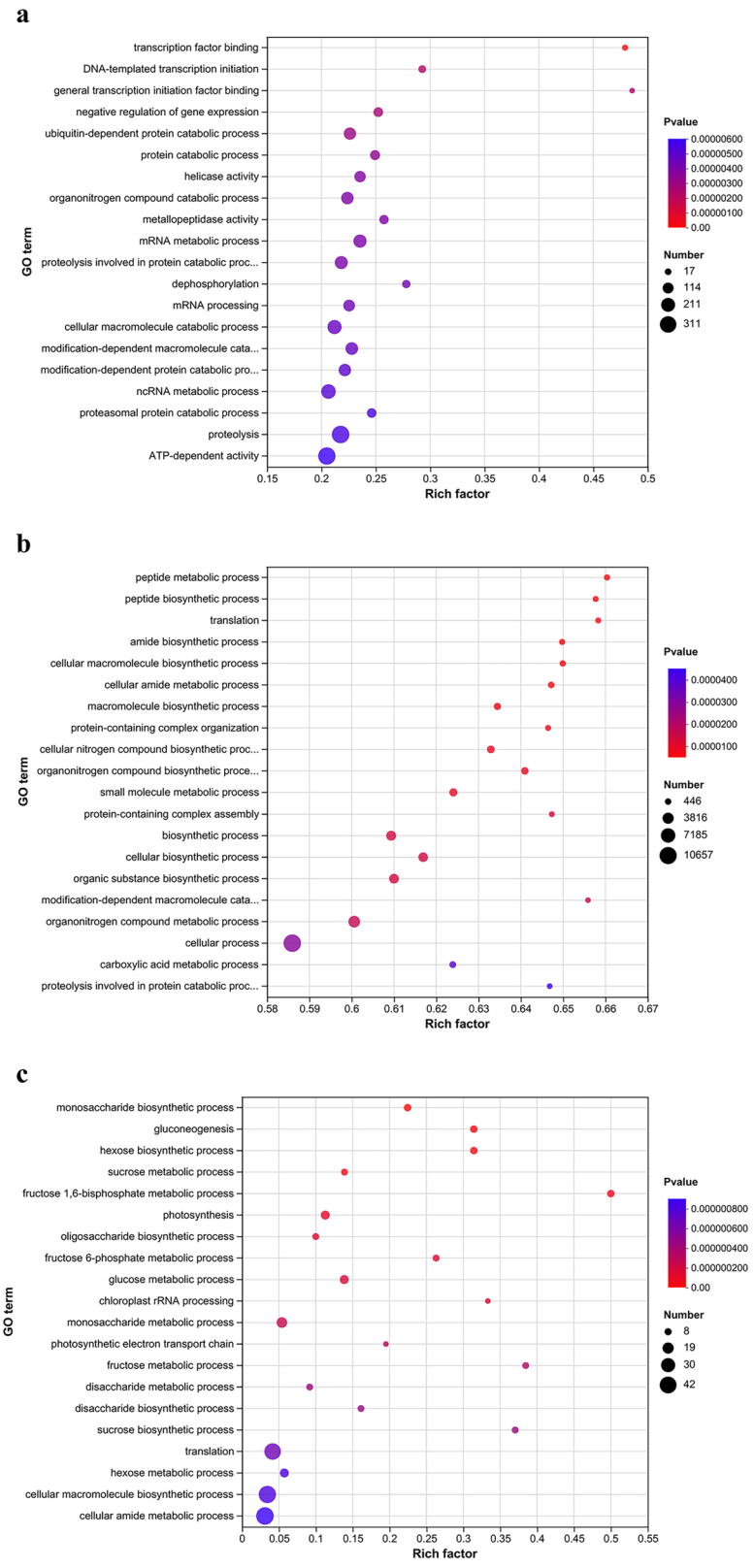

Fig. 6 The top 20 significantly enriched GO terms in turquoise (**a**), steelblue (**b**), and salmon (**c**) module

expressed after inhibitor treatment for 8 h. There were 14 and 17 pathways are associated with energy metabolism in steelblue and salmon module. Analysis of the expression profiles of the top 10 hub genes in the steelblue and salmon modules revealed that the peak expression of these genes occurred at hour 10 (Fig. S3b-c). The results indicated that

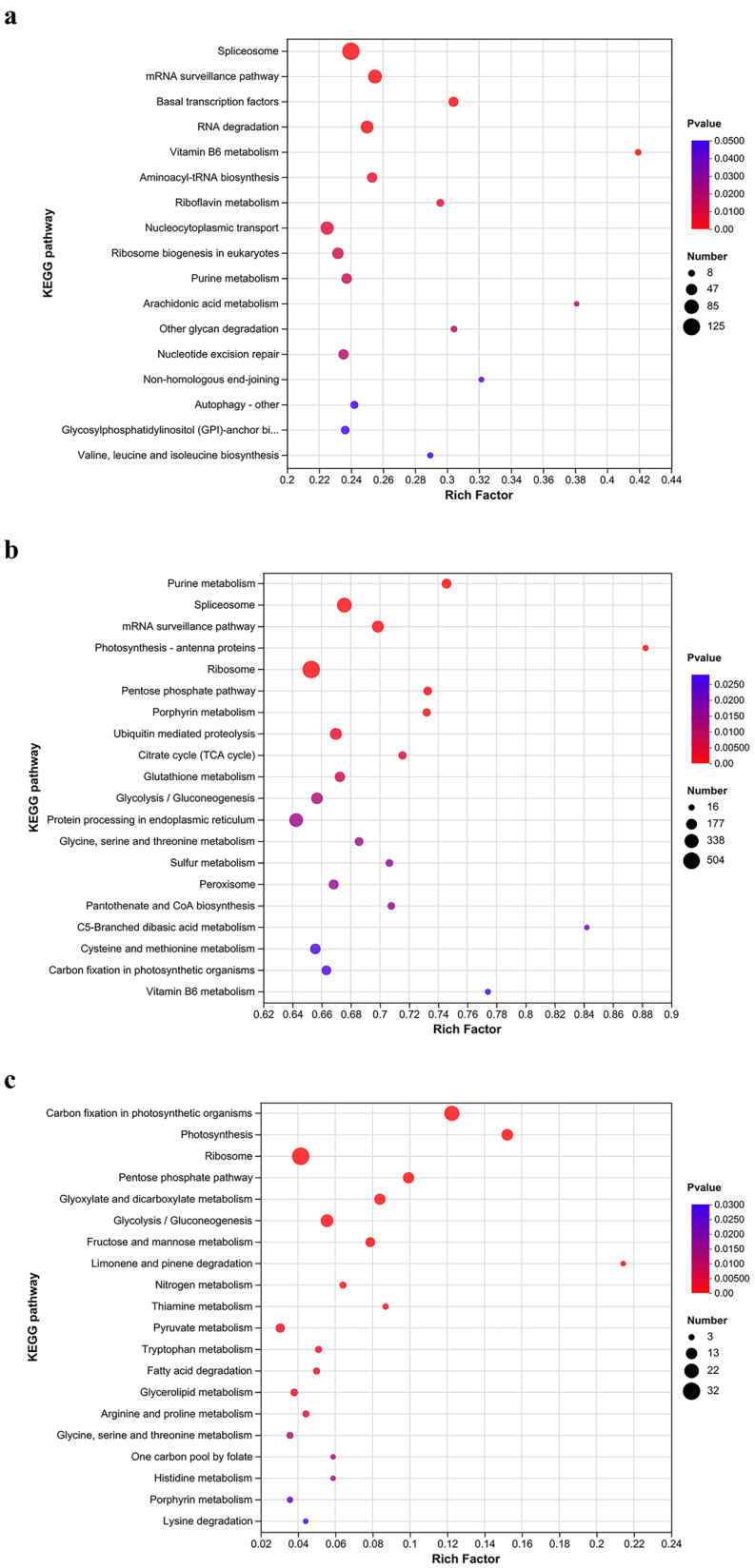

Fig. 7 The top 20 significantly enriched KEGG pathways in turquoise (**a**), steelblue (**b**), and salmon (**c**) module

the genes in the energy metabolism pathway were actively expressed after 10 h of inhibitor treatment.

The multi-to-multi relationship between TFs and target genes

Unlike the GCN, the GRN can be used to study the regulatory relationships between genes. It is known that gene regulation occurs in the nucleus, and the proteins encoded by these genes play roles in various subcellular locations. GO organizes biological knowledge about cell components hierarchically. This makes GRNs analysis not only interpretable mechanistically but also provides new mechanistic insights (Bechtel 2020). Therefore, when constructing the GRNs, DEGs were first classified into five gene sets based on GO subcellular localization annotations. The GO terms of these five gene sets are related to "chloroplast", "mitochondria", "endoplasmic reticulum", "Golgi apparatus", and "cytoplasmic lysosomal". Five GRNs were constructed based on these five gene sets and differentially expressed TFs (Fig. 8; Fig. S4). The top 5 hub genes in each network were identified. Among them, because there were few genes annotated to endoplasmic reticulum, only one central gene was finally screened (Table S8).

The target genes of these specific regulators are involved in various biological pathways (Table S9). For example, in the chloroplast gene regulatory module, *Sm*WRKY48 targeted genes involved in fatty acid biosynthesis, pyruvate metabolism, photosynthesis, arginine biosynthesis, and other pathways. In the mitochondrial gene regulatory module, the target genes of *Sm*AGL16 were involved in various pathways, such as nicotinate and nicotinamide metabolism, pantothenate and CoA biosynthesis, amino acid metabolism and degradation, aminoacyl-tRNA biosynthesis, folate biosynthesis, and other biological processes. In the cytoplasmic lysate gene regulatory module, *Sm*WRKY28 targeted genes involved in glutathione metabolism, pyruvate metabolism, cysteine and methionine metabolism, and glycolysis/gluconeogenesis pathways. Similarly, in *A.thaliana*, the homologous genes of these TFs also exhibit the behavior of targeting genes involved in various biological processes. For example, *At*WRKY48, a homologous gene of *Sm*WRKY48, targeted *At*ASP, *At*IAA2, and *At*DLDG1 in *A.thaliana* acclimation to a combination of high light and heat stress; *At*AGL16, a homologous gene of *Sm*AGL16, regulated the expression of *At*HKT1;1, *At*HsfA6a, and *At*MYB102 in *A.thaliana* salt stress response; *At*WRKY28, a homologous gene of *Sm*WRKY28, targeted genes in the salicylic acid and jasmonic acid/ethylene-dependent defense pathways in *A.thaliana* streptococcus bacteriophage and oxalic acid stress response (Balfagón et al. 2024; Zhao et al. 2021; Chen et al. 2013).

TFs, as a regulatory center, regulate *S.miltiorrhiza* responses to MVA pathway interference by integrating various biological pathways. In the cytoplasmic lysate gene regulatory network, *Sm*WRKY48-*Sm*TCP4-*Sm*WRKY28 worked as a regulation hub to integrate various biological processes, including pyruvate metabolism, glycolysis/gluconeogenesis, amino acid metabolism, and ubiquinone and other terpenoid-quinone biosynthesis (Fig. 8).

In order to further verify whether the identified TFs have a specific response to LOV, the expression profiles of the hub TFs were analyzed after treatment with different concentrations of LOV. It was found that the fluctuation of *Sm*WRKY28 gene expression level was the most obvious, and the coefficient of variation (CV) was 0.396 (Fig. 9). The gene expression levels of *Sm*AGL16 (CV = 0.348), *Sm*ERF1A.1 (CV = 0.333), and

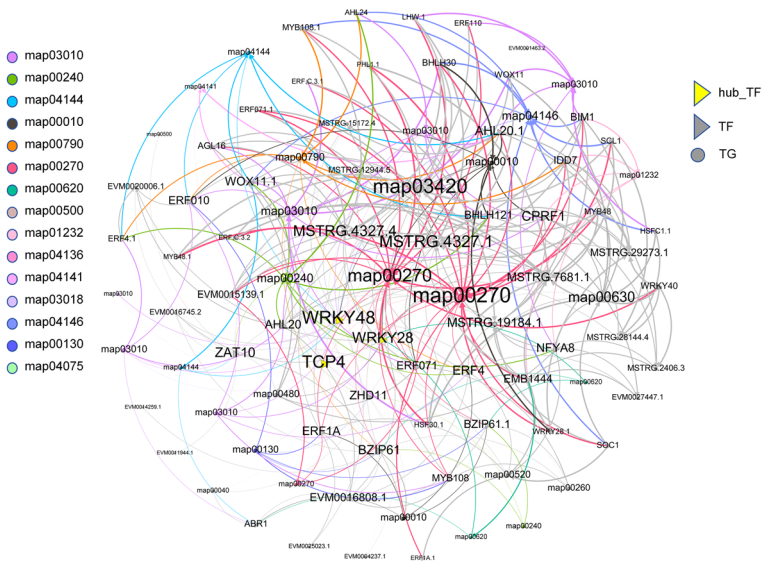

Fig. 8 GRNs constructed based on differentially expressed TFs and DEGs of cytoplasmic lysosomal gene sets ▲: denoting the regulating factors (TFs), ●: denoting the target genes (DEGs); ▲ (highlighted): denoting hub TFs, ●(different colors): denoting DEGs in different biological pathways

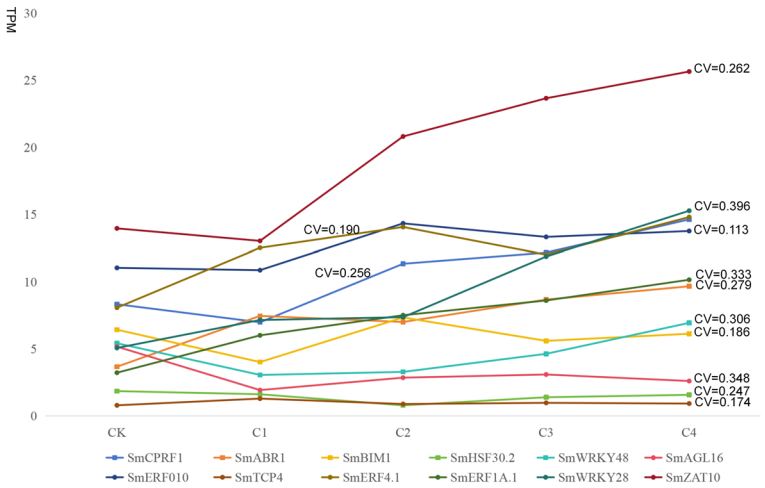

Fig. 9 Expression profiles of hub genes of five GRNs after treatment with different concentrations of LOV CK: control; C1-C4: samples which were collected from MS medium containing the LOV final working solution concentrations of 10 μM, 50 μM, 100 μM, and 200 μM; CV: coefficient of variation

*Sm*WRKY48 (CV = 0.306) fluctuated obviously (Fig. 9). The *Sm*ERF010 (CV = 0.113), *Sm*TCP4 (CV = 0.174), *Sm*BIM1 (CV = 0.186), and *Sm*ERF4.1 (CV = 0.190) gene expression levels tended to be stable (Fig. 9). The gene standardized expression values are presented in the Table S10. In the cytoplasmic lysate gene regulatory network, the gene expression levels of *Sm*WRKY28 and *Sm*WRKY48 fluctuated obviously, while *Sm*TCP4 gene expression level tended to be stable without dramatic fluctuations. It means that *Sm*WRKY28 and *Sm*WRKY48 specifically responded to LOV treatment, while *Sm*TCP4 was not the specific response gene of experimental treatment.

In this study, it was relatively common that a target gene was regulated by several transcription factors. For example, in the chloroplast gene regulatory module, the gene *Sm*PSBR, which is involved in the photosynthesis pathway, was simultaneously targeted by the transcription factors *Sm*CPRF1, *Sm*ABR1, and *Sm*WRKY48. In the mitochondrial gene regulatory module, the gene *Sm*PDL2, which is involved in the folate biosynthesis pathway, was targeted by the transcription factors *Sm*WRKY48, *Sm*AGL16, and *Sm*ERF010.

Validation of RNA-Seq sequencing data by RT-qPCR analysis

To validate the reliability of transcriptome sequencing data, 10 genes were selected for expression correlation analysis: DXS, HMGS, HMGR, IDI, KSL, GA3, CPRF1, TCP4, WRKY40, and WRKY48. The results indicate that the majority of the selected genes displayed expression patterns consistent with the results of transcriptome sequencing, affirming the credibility of our transcriptome data (Fig. S5).

Discussion

Perturbation of essential biological pathways in plants leads to consequences on both their primary and secondary metabolic pathways. In the current study, by perturbing the MVA pathway in *S.miltiorrhiza*, we observed significant differential expression of genes involved in plant primary metabolic processes, such as energy metabolism, carbohydrate metabolism, amino acid metabolism, and lipid compound metabolism. Moreover, genes associated with plant secondary metabolic processes, including terpene and polyketide metabolism, also showed significant differential expression (Fig. 3). The results of the GCNs analysis indicated that genes in the steelblue module and salmon module exhibit significant enrichment for biological processes associated with primary metabolism, such as carbon fixation in photosynthetic organisms, pyruvate metabolism, and glycolysis/gluconeogenesis (Fig. 7). Multiple established studies have also demonstrated that perturbing a specific biological pathway in plants can have implications for several other related biological processes. For example, in *A.thaliana*, interference with the histidine biosynthesis pathway not only blocked histidine biosynthesis but also impacted aromatic amino acids (such as histidine, lysine, and purine) and the tryptophan biosynthesis pathway (Guyer et al. 1995). After treating pear fruit (cv. "Blanquilla") with LOV, various biological processes were influenced, including the metabolism of ascorbic acid, the biosynthesis of phenolic compounds, and lipid biosynthesis (Giné-Bordonaba et al. 2020). When the photosynthetic biological processes of *Oryza sativa* were disturbed, not only was the photosynthetic pathway affected, but also oxidation/reduction-related biological processes were significantly impacted (Hu et al. 2024). Overexpression of APR2, a gene in the sulfate reduction assimilation pathway in *A.thaliana*, promoted the biosynthesis of glutathione and phytochelatins (Xu et al. 2020). Perturbation of the jasmonic

acid biosynthesis pathway in *Oryza sativa* revealed that the processes of sugar metabolism, cell wall biosynthesis, and diurnal flowering time were impacted (Wang et al. 2024).

Perturbation of the MVA pathway in *S.miltiorrhiza* affected several biological processes at different time points. In the early stage (2–6 h), it mainly affected biological processes related to plant growth and development, such as the cell cycle, morphogenesis, and photosynthesis. However, in the late period (8–12 h), it primarily impacted biological processes associated with stress response, including systemic acquired resistance, osmotic stress, water stress, oxidative stress, and cold stress (Fig. 2). Time-dependent changes in transcript expression profiles have also been observed in other plants. For instance, the functional analysis of genes responding at different time points during progressive drought in *A.thaliana* revealed that early DEGs were associated with biological processes such as carbohydrate and glycoside biosynthesis, while late DEGs were involved in flavonoid and pigment biosynthesis (Bechtold et al. 2016). The results of a time-series transcriptome analysis of *Populus* in response to salt stress revealed that it primarily impacted the plant photosynthesis process in the early stage. Subsequently, it triggered the stress resistance response, activated hormone signaling pathways, and influenced flavonoid biosynthesis and metabolism-related processes in the middle and late stages (Zhao et al. 2023). After 2 h of cold treatment in *Ricinus communis*, the DEGs were primarily associated with plant pathogen interactions and autophagy regulation processes. Subsequently, the DEGs were linked to plant circadian rhythms and hormone signaling processes following cold treatment for 6 and 8 h (Wang et al. 2022a, b). Salt stress treatment was observed to primarily impact biological processes associated with plant hormone metabolism during the early stage of stress (6 h) and photosynthesis-related biological processes during the later stage (7 days) in *Vitis vinifera* (Upadhyay et al. 2018).

The changes in biological processes resulting from LOV treatment, occurring at various time intervals, are linked to the topological arrangement of these pathways in the KEGG diagram. This investigation demonstrated that DEGs at different time points were connected to specific terpenoid biosynthesis pathways. For instance, the DEGs were associated with specific biological processes at different time points: monoterpenoid biosynthesis at 2 h, diterpenoid biosynthesis and zeatin biosynthesis at 4 h, carotenoid biosynthesis at 6 h, and terpenoid backbone biosynthesis as well as sesquiterpenoid and triterpenoid biosynthesis at 10 h (Table S11). By perturbing the MVA pathway, the biosynthesis pathways for monoterpenoids, diterpenoids, zeatin, and carotenoids, located downstream of the terpenoid backbone biosynthesis pathway, were notably influenced at the early stage. Subsequently, genes in the MVA pathway and MEP pathway, which are situated upstream of the terpenoid backbone biosynthesis pathway, were significantly affected at a later time point (Fig. 10). It has been reported that the inhibition of HMGR activity using LOV led to decreased expression levels of genes downstream of the terpenoid backbone biosynthesis pathway, including MK, PMK, DPMD, SLS, and STR (Rather et al. 2019). Our study reveals the sequence of the affected biosynthetic pathways when the MVA pathway in *S.miltiorrhiza* was perturbated by an inhibitor. It is closely associated with the topological relationships between these biosynthetic pathways.

TFs often act as the regulatory hubs regulating plant responses to stress through mediating synergistic interactions among distinct biological processes in plants. The constructed GRNs in this study demonstrated that TFs targeted genes from multiple biological pathways. In this study, a transcription factor combination, *Sm*WRKY48-*Sm*TCP4-*Sm*WRKY28, was found in the cytoplasmic lysate gene regulatory network. *Sm*WRKY48-*Sm*TCP4-*Sm*WRKY28 targeted genes involved in pyruvate metabolism, glycolysis/gluconeogenesis, amino acid metabolism, and ubiquinone and other terpenoid-quinone biosynthesis (Fig. 8). Research has also demonstrated that WRKY genes can regulate plant stress tolerance by acting in conjunction with other TFs. For example, *At*WRKY18, *At*WRKY40 and *At*WRKY60 TFs form a highly interacting regulatory network that modulates gene expression in *A.thaliana* responses to abscisic acid and abiotic stress (Chen et al. 2010). *At*WRKY70 and *At*WRKY54 co-operate as negative regulators of the osmotic stress response in *A.thaliana* (Li et al. 2013). *Pe*HSF-*Pe*WRKY1 regulated the K^+/Na^+ homeostasis under high-salinity conditions in *Populus euphratica* (Shen et al. 2015).

The dynamic combination of different TFs endows plants with robustness to adapt to the environment in different situations. Studies have shown that multiple TFs were involved in the response of plants to environmental stress (Meng et al. 2024). In this study, we analyzed the expression profiles of the hub transcription factor combination *Sm*WRKY48-*Sm*TCP4-*Sm*WRKY28, and found that *Sm*WRKY48 and *Sm*WRK28 were the inhibitor-specific response factors, while *Sm*TCP4 was a nonspecific response factor. Previous studies have shown that the members of TCP TFs family, a plant-specific transcription factors, are involved in a broad range of physiological processes of plant growth and development (Wang et al. 2022a, b). They mainly regulate the process of plant cell division and differentiation (Martín-Trillo and Cubas 2010). We speculate that *Sm*TCP4 may play a conservative role in maintaining the normal growth of plants in *S.miltiorrhiza*. Therefore, the expression of *Sm*TCP4 did not change significantly during 12 h of LOV treatment with different concentrations. The WRKY family are widely known to respond to biotic and abiotic stresses, and participates in the adaptive response of

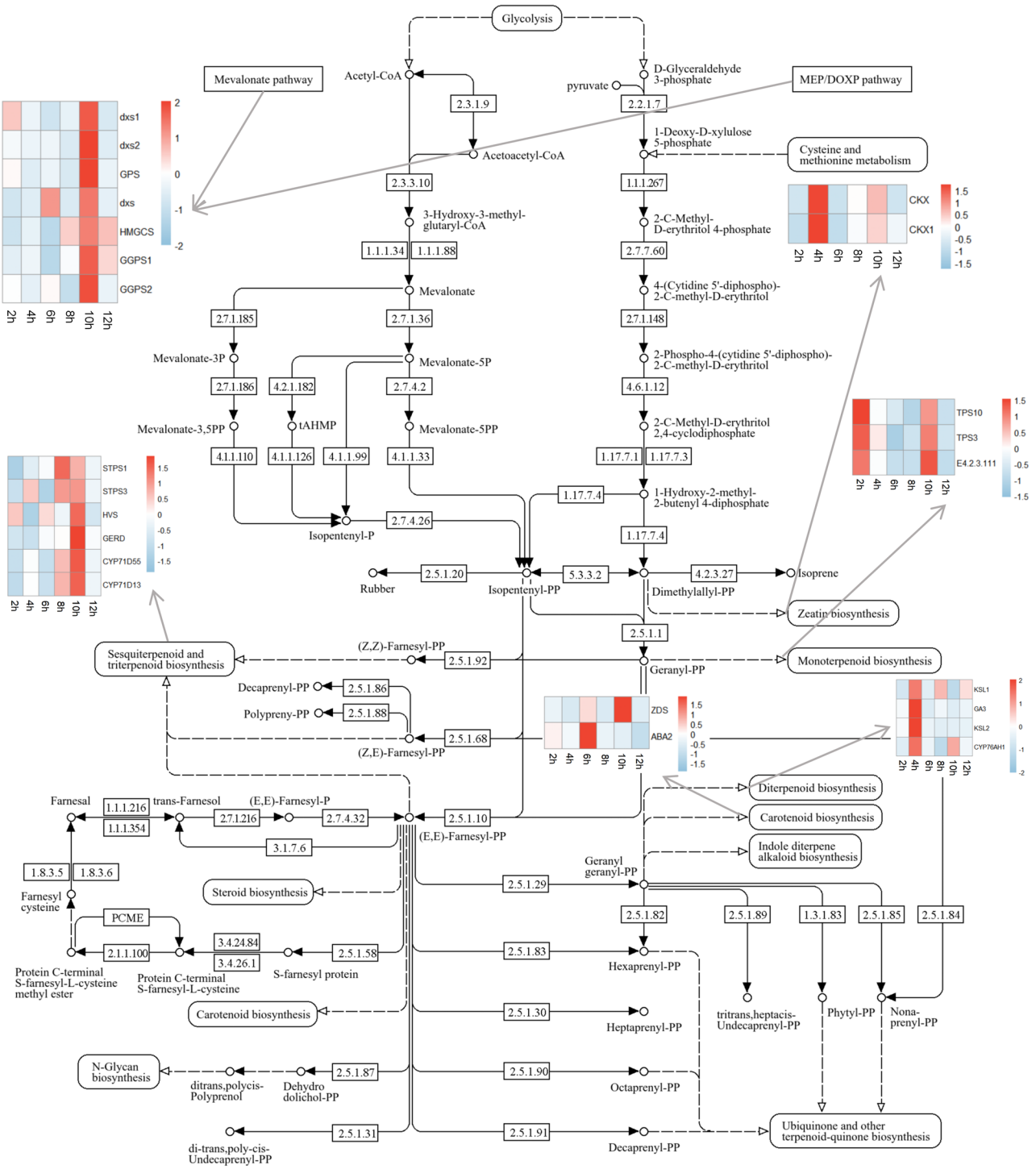

Fig. 10 Diagram of terpenoid backbone biosynthesis pathways (taken from KEGG website http: //www.genome.jp/kegg). The heatmap shows the | log2 (fold change) | value of differentially expressed genes in different terpenoid biosynthesis pathways. The locations marked by heatmap in the figure are the pathways significantly enriched for differentially expressed genes at different time points

plants (Rushton et al. 2010). In *S.miltiorrhiza*, *Sm*WRKY48 and *Sm*WRK28 may be the key response factors of LOV treatment, and cooperated with *Sm*TCP4 to form the regulatory hub of this gene regulatory network.

Conclusion

Our findings suggest that perturbation of a key biological pathway in *S.miltiorrhiza* has time-dependent effects on

other biological processes. In general, the growth and development processes of *S.miltiorrhiza* are primarily affected at the early stage, whereas stress response-related biological processes are mainly influenced at the later stage. Additionally, pathways, located downstream of the terpenoid backbone biosynthesis pathway, are predominantly affected at the early stage. The MVA and MEP pathways are impacted at the later stage. This suggests that the order of the affected biosynthetic pathways is associated with the topological distribution of these biological pathways. The GRNs based on TFs indicated that *Sm*WRKY48-*Sm*TCP4-*Sm*WRKY28 worked as a regulation hub to integrate synergistic interactions among distinct biological processes in *S.miltiorrhiza.* These findings provide insights for a deeper understanding of the molecular mechanisms through which various biological processes synergistically interact.

Supplementary Information The online version contains supplementary material available at https://doi.org/10.1007/s11103-024-01547-5.

Acknowledgements Not applicable.

Author contributions All authors contributed to the study conception and design. LF conceived, designed, performed the experiments and data analysis, and wrote the manuscript. LN contributed to data analysis and manuscript writing. YZY conceived and designed experiments, wrote or reviewed drafts of papers. CX conceived and designed experiments, wrote or reviewed drafts of papers. All authors contributed to the article and approved the submitted version.

Funding This study was funded by the National Natural Science Foundation of China (82373984). Natural Science Foundation of China: 82373984.

Data availability All data supporting the findings of this study are included in this manuscript and its supplementary files or further materials can be obtain from the corresponding author upon request. The transcriptome sequencing data that support the findings of this study have been deposited in NCBI Sequence Read Archive with the accession code PRJNA1111691 and PRJNA1112563. Source data are provided with this paper.

Declarations

Conflict of interest The authors declare no competing financial interests.

Ethical approval Not applicable.

Consent for publication Not applicable.

References

Almeida-Silva F, Venancio TM (2022) BioNERO: an all-in-one R/Bioconductor package for comprehensive and easy biological network reconstruction. Funct Integr Genomics 22(1):131–136. https://doi.org/10.1007/s10142-021-00821-9

Alvarez JM, Brooks MD, Swift J, Coruzzi GM (2021) Time-based systems biology approaches to capture and model dynamic gene regulatory networks. Annu Rev Plant Biol 72:105–131. https://doi.org/10.1146/annurev-arplant-081320-090914

Bai Y, Yu H, Chen L, Meng Y, Ma Y, Wang D, Qian Y, Zhang D, Feng X, Zhou Y (2023) Time-course transcriptome analysis of *Aquilegia vulgaris* root reveals the cell wall’s roles in salinity tolerance. Int J Mol Sci 24:16450

Balfagón D, Pascual LS, Sengupta S, Halliday KJ, Gómez-Cadenas A, Peláez-Vico M, Sinha R, Mittler R, Zandalinas SI (2024) WRKY48 negatively regulates plant acclimation to a combination of high light and heat stress. Plant J 117:1642–1655. https://doi.org/10.1111/tpj.16658

Bastian M, Heymann S, Jacomy M (2009) Gephi: An open source software for exploring and manipulating networks.

Bechtel W (2020) Hierarchy and levels: analysing networks to study mechanisms in molecular biology. Philos Trans R Soc Lond B Biol Sci 375:20190320. https://doi.org/10.1098/rstb.2019.0320

Bechtold U, Penfold CA, Jenkins DJ, Legaie R, Moore JD, Lawson T, Matthews JSA, Vialet-Chabrand SRM, Baxter L, Subramaniam S, Hickman R, Florance H, Sambles C, Salmon DL, Feil R, Bowden L, Hill C, Baker NR, Lunn JE, Finkenstädt B, Mead A, Buchanan-Wollaston V, Beynon J, Rand DA, Wild DL, Denby KJ, Ott S, Smirnoff N, Mullineaux PM (2016) Time-series transcriptomics reveals that AGAMOUS-LIKE22 affects primary metabolism and developmental processes in drought-stressed Arabidopsis. Plant Cell 28:345–366. https://doi.org/10.1105/tpc.15.00910

Blazquez MA, Yang D, Du X, Liang X, Han R, Liang Z, Liu Y, Liu F, Zhao J (2012) Different roles of the mevalonate and methylerythritol phosphate pathways in cell growth and tanshinone production of *Salvia miltiorrhiza* hairy roots. PLoS One. https://doi.org/10.1371/journal.pone.0046797

Cao L, Zhou Z, Sun J, Li C, Zhang Y (2021) Altering sterol composition implied that cholesterol is not physiologically associated with diosgenin biosynthesis in *Trigonella foenum-graecum*. Frontiers in Plant Science. https://doi.org/10.3389/fpls.2021.741604

Chen H, Lai Z, Shi J, Xiao Y, Chen Z, Xu X (2010) Roles of arabidopsis WRKY18, WRKY40 and WRKY60 transcription factors in plant responses to abscisic acid and abiotic stress. BMC Plant Biol 10(1):281. https://doi.org/10.1186/1471-2229-10-281

Chen X, Liu J, Lin G, Wang A, Wang Z, Lu G (2013) Overexpression of AtWRKY28 and AtWRKY75 in Arabidopsis enhances resistance to oxalic acid and Sclerotinia sclerotiorum. Plant Cell Rep 32:1589–1599. https://doi.org/10.1007/s00299-013-1469-3

Chen S, Zhou Y, Chen Y, Gu J (2018) fastp: an ultra-fast all-in-one FASTQ preprocessor. Bioinformatics 34(17):i884–i890. https://doi.org/10.1093/bioinformatics/bty560

Chin CH, Chen SH, Wu HH, Ho CW, Ko MT, Lin CY (2014) cytoHubba: identifying hub objects and sub-networks from

complex interactome. BMC Syst Biol. https://doi.org/10.1186/1752-0509-8-s4-s11
Cho S-H, Tóth K, Kim D, Vo PH, Lin C-H, Handakumbura PP, Ubach AR, Evans S, Paša-Tolić L, Stacey G (2022) Activation of the plant mevalonate pathway by extracellular ATP. Nat Commun. https://doi.org/10.1038/s41467-022-28150-w
Faith JJ, Hayete B, Thaden JT, Mogno I, Wierzbowski J, Cottarel G, Kasif S, Collins JJ, Gardner TS (2007) Large-scale mapping and validation of *Escherichia coli* transcriptional regulation from a compendium of expression profiles. PLoS Biol 5(1):e8. https://doi.org/10.1371/journal.pbio.0050008
Gao W, Sun HX, Xiao H, Cui G, Hillwig ML, Jackson A, Wang X, Shen Y, Zhao N, Zhang L, Wang XJ, Peters RJ, Huang L (2014) Combining metabolomics and transcriptomics to characterize tanshinone biosynthesis in *Salvia miltiorrhiza*. BMC Genomics 15:73. https://doi.org/10.1186/1471-2164-15-73
Giné-Bordonaba J, Busatto N, Larrigaudière C, Lindo-García V, Echeverria G, Vrhovsek U, Farneti B, Biasioli F, De Quattro C, Rossato M, Delledonne M, Costa F (2020) Investigation of the transcriptomic and metabolic changes associated with superficial scald physiology impaired by lovastatin and 1-methylcyclopropene in pear fruit (cv. "Blanquilla"). Hortic Res 7(1):49. https://doi.org/10.1038/s41438-020-0272-x
Guyer D, Patton D, Ward E (1995) Evidence for cross-pathway regulation of metabolic gene expression in plants. Proc Natl Acad Sci 92:4997–5000. https://doi.org/10.1073/pnas.92.11.4997
Hagen C, Grunewald K (2000) Fosmidomycin as an inhibitor of the non-mevalonate terpenoid pathway depresses synthesis of secondary carotenoids in flagellates of the green alga Haematococcus pluvialis. J Appl Botany-Angewandte Botanik 74:137–140
Haury AC, Mordelet F, Vera-Licona P, Vert JP (2012) TIGRESS: trustful inference of gene REgulation using stability selection. BMC Syst Biol 6:145. https://doi.org/10.1186/1752-0509-6-145
Hu Y, Tian C, Song S, Li R (2024) Insights on the enhancement of chilling tolerance in rice through over-expression and knock-out studies of OsRBCS3. Plant Signal Behav 19(1):2318514. https://doi.org/10.1080/15592324.2024.2318514
Huynh-Thu VA, Irrthum A, Wehenkel L, Geurts P (2010) Inferring regulatory networks from expression data using tree-based methods. PLoS One. https://doi.org/10.1371/journal.pone.0012776
Jiang T, Zhang M, Wen C, Xie X, Tian W, Wen S, Lu R, Liu L (2020) Integrated metabolomic and transcriptomic analysis of the anthocyanin regulatory networks in *Salvia miltiorrhiza* Bge. flowers. BMC Plant Biol 20:349. https://doi.org/10.1186/s12870-020-02553-7
Kanehisa M, Goto S (2000) KEGG: Kyoto encyclopedia of genes and genomes. Nucleic Acids Res 28(1):27–30. https://doi.org/10.1093/nar/28.1.27
Kanehisa M, Araki M, Goto S, Hattori M, Hirakawa M, Itoh M, Katayama T, Kawashima S, Okuda S, Tokimatsu T, Yamanishi Y (2008) KEGG for linking genomes to life and the environment. Nucleic Acids Res 36:D480–D484. https://doi.org/10.1093/nar/gkm882
Kim D, Langmead B, Salzberg SL (2015) HISAT: a fast spliced aligner with low memory requirements. Nat Methods 12(4):357–360. https://doi.org/10.1038/nmeth.3317
Kong D, Li C, Xue W, Wei H, Ding H, Hu G, Zhang X, Zhang G, Zou T, Xian Y, Wang B, Zhao Y, Liu Y, Xie Y, Xu M, Wu H, Liu Q, Wang H (2023) UB2/UB3/TSH4-anchored transcriptional networks regulate early maize inflorescence development in response to simulated shade. Plant Cell 35:717–737. https://doi.org/10.1093/plcell/koac352
Krause T, Wiesinger P, González-Cabanelas D, Lackus N, Köllner TG, Klüpfel T, Williams J, Rohwer J, Gershenzon J, Schmidt A (2023) HDR, the last enzyme in the MEP pathway, differently regulates isoprenoid biosynthesis in two woody plants. Plant Physiol 192(2):767–788. https://doi.org/10.1093/plphys/kiad110
Langfelder P, Horvath S (2008) WGCNA: an R package for weighted correlation network analysis. BMC Bioinformatics 9:559. https://doi.org/10.1186/1471-2105-9-559
Li B, Dewey CN (2011) RSEM: accurate transcript quantification from RNA-Seq data with or without a reference genome. BMC Bioinformatics 12:323. https://doi.org/10.1186/1471-2105-12-323
Li J, Besseau S, Törönen P, Sipari N, Kollist H, Holm L, Palva ET (2013) Defense-related transcription factors WRKY70 and WRKY54 modulate osmotic stress tolerance by regulating stomatal aperture in Arabidopsis. New Phytol 200:457–472. https://doi.org/10.1111/nph.12378
Li C-F, Zhu Y, Yu Y, Zhao Q-Y, Wang S-J, Wang X-C, Yao M-Z, Luo D, Li X, Chen L, Yang Y-J (2015a) Global transcriptome and gene regulation network for secondary metabolite biosynthesis of tea plant (*Camellia sinensis*). BMC Genomics 16(1):560. https://doi.org/10.1186/s12864-015-1773-0
Li Y, Varala K, Coruzzi GM (2015b) From milliseconds to lifetimes: tracking the dynamic behavior of transcription factors in gene networks. Trends Genet 31:509–515. https://doi.org/10.1016/j.tig.2015.05.005
Livak KJ, Schmittgen TD (2001) Analysis of relative gene expression data using real-time quantitative PCR and the 2(-Delta Delta C(T)) Method. Methods 25(4):402–408. https://doi.org/10.1006/meth.2001.1262
Love MI, Huber W, Anders S (2014) Moderated estimation of fold change and dispersion for RNA-seq data with DESeq2. Genome Biol 15(12):550. https://doi.org/10.1186/s13059-014-0550-8
Lu LL, Zhang YX, Yang YF (2022) Integrative transcriptomic and metabolomic analyses unveil tanshinone biosynthesis in Salvia miltiorrhiza root under N starvation stress. PLoS One 17(8):e0273495. https://doi.org/10.1371/journal.pone.0273495
Marbach D, Costello JC, Küffner R, Vega NM, Prill RJ, Camacho DM, Allison KR, Aderhold A, Allison KR, Bonneau R, Camacho DM, Chen Y, Collins JJ, Cordero F, Costello JC, Crane M, Dondelinger F, Drton M, Esposito R, Foygel R, de la Fuente A, Gertheiss J, Geurts P, Greenfield A, Grzegorczyk M, Haury A-C, Holmes B, Hothorn T, Husmeier D, Huynh-Thu VA, Irrthum A, Kellis M, Karlebach G, Küffner R, Lèbre S, De Leo V, Madar A, Mani S, Marbach D, Mordelet F, Ostrer H, Ouyang Z, Pandya R, Petri T, Pinna A, Poultney CS, Prill RJ, Rezny S, Ruskin HJ, Saeys Y, Shamir R, Sîrbu A, Song M, Soranzo N, Statnikov A, Stolovitzky G, Vega N, Vera-Licona P, Vert J-P, Visconti A, Wang H, Wehenkel L, Windhager L, Zhang Y, Zimmer R, Kellis M, Collins JJ, Stolovitzky G, The DC (2012) Wisdom of crowds for robust gene network inference. Nat Methods 9:796–804. https://doi.org/10.1038/nmeth.2016
Margolin AA, Nemenman I, Basso K, Wiggins C, Stolovitzky G, Favera RD, Califano A (2006) ARACNE: An algorithm for the reconstruction of gene regulatory networks in a mammalian cellular context. BMC Bioinformatics 7(1):S7. https://doi.org/10.1186/1471-2105-7-S1-S7
Martín-Trillo M, Cubas P (2010) TCP genes: a family snapshot ten years later. Trends Plant Sci 15(1):31–39. https://doi.org/10.1016/j.tplants.2009.11.003
Meng S, Yan X, Piao Y, Li S, Wang X, Jiang J, Liang Y, Pang W (2024) Multiple transcription factors involved in the response of Chinese cabbage against Plasmodiophora brassicae. Front Plant Sci 15:1391173. https://doi.org/10.3389/fpls.2024.1391173
Murashige T, Skoog FK (1962) A revised medium for rapid growth and bio assays with tobacco tissue cultures. Physiol Plant 15:473–497
Pichersky E, Raguso RA (2018) Why do plants produce so many terpenoid compounds? New Phytol 220(3):692–702. https://doi.org/10.1111/nph.14178
Rather GA, Sharma A, Jeelani SM, Misra P, Kaul V, Lattoo SK (2019) Metabolic and transcriptional analyses in response to potent inhibitors establish MEP pathway as major route for camptothecin

biosynthesis in Nothapodytes nimmoniana (Graham) Mabb. BMC Plant Biol 19(1):301. https://doi.org/10.1186/s12870-019-1912-x

Rohmer M, Rohmer M (1999) The discovery of a mevalonate-independent pathway for isoprenoid biosynthesis in bacteria, algae and higher plants†. Nat Prod Rep 16(5):565–574. https://doi.org/10.1039/a709175c

Rushton PJ, Somssich IE, Ringler P, Shen QJ (2010) WRKY transcription factors. Trends Plant Sci 15:247–258. https://doi.org/10.1016/j.tplants.2010.02.006

Shannon P, Markiel A, Ozier O, Baliga NS, Wang JT, Ramage D, Amin N, Schwikowski B, Ideker T (2003) Cytoscape: a software environment for integrated models of biomolecular interaction networks. Genome Res 13:2498–2504. https://doi.org/10.1101/gr.1239303

Shen Z, Yao J, Sun J, Chang L, Wang S, Ding M, Qian Z, Zhang H, Zhao N, Sa G, Hou P, Lang T, Wang F, Zhao R, Shen X, Chen S (2015) Populus euphratica HSF binds the promoter of WRKY1 to enhance salt tolerance. Plant Sci 235:89–100. https://doi.org/10.1016/j.plantsci.2015.03.006

Shen-Orr SS, Milo R, Mangan S, Alon U (2002) Network motifs in the transcriptional regulation network of Escherichia coli. Nat Genet 31(1):64–68. https://doi.org/10.1038/ng881

Singh VK, Mangalam AK, Dwivedi S, Naik S (1998) Primer premier: program for design of degenerate primers from a protein sequence. Biotechniques 24(2):318–319. https://doi.org/10.2144/98242pf02

Song Z, Lin C, Xing P, Fen Y, Jin H, Zhou C, Gu YQ, Wang J, Li X (2020) A high-quality reference genome sequence of Salvia miltiorrhiza provides insights into tanshinone synthesis in its red rhizomes. Plant Genome 13:e20041. https://doi.org/10.1002/tpg2.20041

Tsai K-L, Chen EG, Chen J-T (2015) Thidiazuron-induced efficient propagation of Salvia miltiorrhiza through in vitro organogenesis and medicinal constituents of regenerated plants. Acta Physiol Plant 38:29. https://doi.org/10.1007/s11738-015-2051-0

Upadhyay A, Gaonkar T, Upadhyay AK, Jogaiah S, Shinde MP, Kadoo NY, Gupta VS (2018) Global transcriptome analysis of grapevine (Vitis vinifera L.) leaves under salt stress reveals differential response at early and late stages of stress in table grape cv. Thompson seedless. Plant Physiol Biochem 129:168–179. https://doi.org/10.1016/j.plaphy.2018.05.032

Wang JL, Wang HW, Cao YN, Kan SL, Liu YY (2022a) Comprehensive evolutionary analysis of the TCP gene family: Further insights for its origin, expansion, and diversification. Front Plant Sci 13:994567. https://doi.org/10.3389/fpls.2022.994567

Wang X, Wu Y, Sun M, Wei X, Huo H, Yu L, Zhang J (2022) Dynamic transcriptome profiling revealed key genes and pathways associated with cold stress in castor (*Ricinus communis* L.). Ind Crops Products 178:114610. https://doi.org/10.1016/j.indcrop.2022.114610

Wang M, Zhu X, Huang Z, Chen M, Xu P, Liao S, Zhao Y, Gao Y, He J, Luo Y, Chen H, Wei X, Nie S, Dong J, Zhu L, Zhuang C, Zhao J, Liu Z, Zhou H (2024) Controlling diurnal flower-opening time by manipulating the jasmonate pathway accelerates development of indica-japonica hybrid rice breeding. Plant Biotechnol J. https://doi.org/10.1111/pbi.14343

Xu Z, Wang M, Xu D, Xia Z (2020) The Arabidopsis APR2 positively regulates cadmium tolerance through glutathione-dependent pathway. Ecotoxicol Environ Saf 187:109819. https://doi.org/10.1016/j.ecoenv.2019.109819

Yang J, Cui W, You Q, Liu M, Liu X, Zhao F, Zhu Y, Duan Y, Xue T, Xue J (2023) Transcriptome analysis reveals long non-coding RNAs involved in shade-induced growth promotion in *Pinellia ternata*. Front Biosci-Landmark. https://doi.org/10.31083/j.fbl2809202

Young MD, Wakefield MJ, Smyth GK, Oshlack A (2010) Gene ontology analysis for RNA-seq: accounting for selection bias. Genome Biol 11(2):R14. https://doi.org/10.1186/gb-2010-11-2-r14

Zhang M, Liu H, Wang Q, Liu S, Zhang Y (2020) The 3-hydroxy-3-methylglutaryl-coenzyme A reductase 5 gene from Malus domestica enhances oxidative stress tolerance in *Arabidopsis thaliana*. Plant Physiol Biochem 146:269–277. https://doi.org/10.1016/j.plaphy.2019.11.031

Zhao M, Li J, Zhu L, Chang P, Li L, Zhang L (2019) Identification and characterization of MYB-bHLH-WD40 regulatory complex members controlling anthocyanidin biosynthesis in blueberry fruits development. Genes (Basel). https://doi.org/10.3390/genes10070496

Zhao PX, Zhang J, Chen SY, Wu J, Xia JQ, Sun LQ, Ma SS, Xiang CB (2021) Arabidopsis MADS-box factor AGL16 is a negative regulator of plant response to salt stress by downregulating salt-responsive genes. New Phytol 232:2418–2439. https://doi.org/10.1111/nph.17760

Zhao Y, Jia K, Tian Y, Han K, El-Kassaby YA, Yang H, Si H, Sun Y, Li Y (2023) Time-course transcriptomics analysis reveals key responses of populus to salt stress. Ind Crops Prod 194:116278. https://doi.org/10.1016/j.indcrop.2023.116278